Density-functional model cluster studies of EPR *g* tensors of F_s^+ centers on the surface of MgO

Cristiana Di Valentin
Dipartimento di Scienza dei Materiali, Università degli Studi Milano-Bicocca, 20125 Milano, Italy

Konstantin M. Neyman[a)]
Institució Catalana de Recerca i Estudis Avançats (ICREA), 08010 Barcelona, Spain and Departament de Química Físisca i Centre especial de Recerca en Química Teòrica, Universitat de Barcelona i Parc Cientific de Barcelona, 08028 Barcelona, Spain

Thomas Risse, Martin Sterrer, Esther Fischbach, and Hans-Joachim Freund
Fritz-Haber Institut der Max-Planck Gesellschaft, Department of Chemical Physics, Faradayweg 4-6, D-14195 Berlin, Germany

Vladimir A. Nasluzov
Institute of Chemistry and Chemical Technology, Russian Academy of Sciences, 660049 Krasnoyarsk, Russia

Gianfranco Pacchioni
Dipartimento di Scienza dei Materiali, Università degli Studi Milano-Bicocca, 20125 Milano, Italy

Notker Rösch
Department Chemie, Theoretische Chemie, Technische Universitat München, 85747 Garching, Germany

(Received 14 October 2005; accepted 1 December 2005; published online 30 January 2006)

We report *g* tensors of surface color centers, so-called F_s^+ centers, of MgO calculated with two density-functional approaches using accurately embedded cluster models. In line with recent UHV measurements on single-crystalline MgO film, we determined only small *g*-tensor anisotropies and negative shifts $\Delta g \equiv g - g_e$ for all F_s^+ sites considered, namely, (001)-terrace, step, edge, and corner sites. The *g* values are very sensitive to the local structure of the defect: relaxation reverses the sign of Δg. However, accounting for the spin-orbit interaction either self-consistently or perturbatively yields very similar results. In addition to the values of the tensor components, their direction with respect to the surface was determined. In contrast to edges, significant deviations from ideal C_{2v} symmetry were found for F_s^+ centers at steps. Recent data on single-crystalline thin films are reevaluated in the light of these results. © *2006 American Institute of Physics*.
[DOI: 10.1063/1.2161190]

I. INTRODUCTION

Oxygen vacancies, or color centers, are considered to play an important role in the reactivity of metal oxide surfaces.[1] However, direct detection of oxygen vacancies is not easy:[1] it has become possible with the help of scanning tunneling microscopy (STM) only recently.[2] Even for such a simple oxide as MgO detailed experimental information on the structure and properties of surface color centers F_s^{n+} ($n=0$, 1, 2) remains limited.[1] F_s^+ vacancies, left behind after removal of O^-, trap a single electron. Thus, electron paramagnetic resonance (EPR) spectroscopy can be used to characterize these sites by their electronic *g*- and hyperfine coupling matrices (commonly referred to as tensors).[3] F_s^+ centers have been studied extensively on polycrystalline MgO samples[4–6] and on MgO films.[7,8] However, a detailed structural understanding of the observed EPR spectra relies on theoretical support as shown for the assignment of $F_s^+(H)$ centers, $(H^+)(e^-)$ pairs, being the main trapping site under certain experimental conditions.[5]

Very recently, EPR spectra of surface color centers taken at the *X* band (10 GHz) have been measured on single-crystalline MgO thin films under ultrahigh-vacuum (UHV) conditions.[9] Thanks to the ordered character of the samples, structural information on F_s^+ centers has been extracted in addition to the careful determination of the principal components of an almost isotropic *g* tensor. (In case of a small anisotropy of *g* tensor, high-field EPR spectroscopy, e.g., at the *W* band (95 GHz), would enhance the resolution of the Zeeman components, thus, providing more accurate *g* values. In addition, it will be advantageous for separating *g* and hyperfine structures.[10,11]) From the analysis of the angular dependence of the line shape, the paramagnetic centers generated by electron bombardment on the surface of MgO thin films were found to be predominantly located at the edges of MgO(001) facets.[9]

In general, the *g*-tensor components contain delicate information on the structure of paramagnetic species, their en-

[a)]Author to whom correspondence should be addressed. Electronic mail: konstantin.neyman@icrea.es

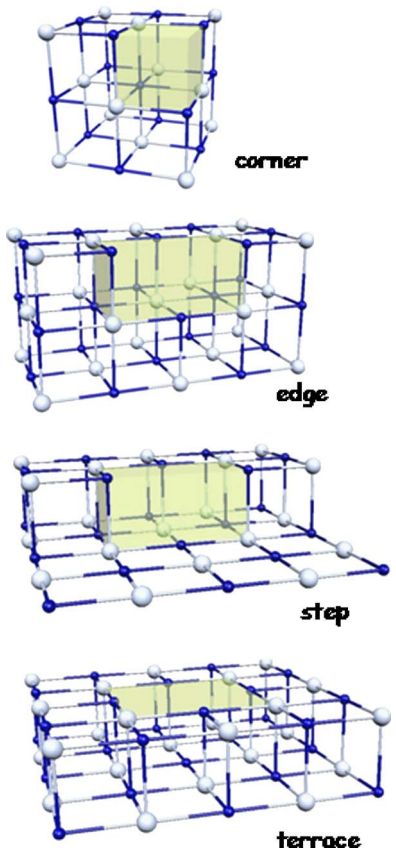

FIG. 1. (Color online) Schematic representation of oxygen vacancies formed on corner, edge, step, and terrace sites of the MgO(100) surface.

vironment as well as on the local behavior of their wave functions.[10] A significant limiting factor, however, is the difficulty to interpret EPR g values in terms of conventional quantities characterizing the electronic structure. To this end, high-level theoretical calculations of the Zeeman structure can help. In fact, the rather complex description of g values in terms of electronic structure parameters requires one to account for various magnetic contributions[12] and to work with sufficiently accurate eigenfunctions. Spin-orbit interaction, which is crucial for quantifying the deviation of g from the free-electron value g_e,[3,12] can be either accounted for self-consistently or treated as a perturbation. The former approach has been elaborated by some of us[13] and implemented in the density-functional (DF) code PARAGAUSS.[14,15] It employs two-component Kohn-Sham (KS) eigenfunctions,[16] obtained with the Douglas-Kroll-Hess[17,18] (DKH) approach to the four-component Dirac-Kohn-Sham problem.[19] Therefore, that method is suitable for treating both light-element radicals (with minor spin-orbit interactions) and heavy atom systems (where spin-orbit effects are large). An example of the spin-orbit perturbation strategy for calculating g tensors is the scheme of Neese,[20] implemented in the code GAUSSIAN03.[21]

In the present work, we employed these two different DF approaches for comparing g-tensor results on F_s^+ centers that are located at various positions of the surface of MgO (Fig. 1). To this end, we studied a series of cluster models optimized when consistently embedded in a polarizable environment by means of two advanced, independently developed embedding schemes.[22,23] We will show that, despite of notable methodological differences, g tensors of the same type of F_s^+ centers, obtained with the different computational approaches under consideration, are very similar and do not show a strong dependence on the exchange-correlation (xc) functional, while they exhibit a dramatic sensitivity to the structure of F_s^+ centers. This limits to some extent the accuracy of calculated g values of F_s^+ centers on MgO, which are only very slightly anisotropic and exhibit very small shifts from g_e. We also analyze recently obtained experimental results on F_s^+ centers generated on the surface of MgO thin films based on the calculations.

II. COMPUTATIONAL DETAILS AND MODELS

In the calculations with the code PARAGAUSS,[14,15] we employed the linear combination of Gaussian-type orbitals fitting-function density-functional method.[24] The geometry optimization was performed at the nonrelativistic level in a spin-polarized fashion. Then, with two-component relativistic wave functions of the Kramers doublet representing the unpaired electron of the F_s^+ center, we calculated g values in the restricted KS approximation.[13] The gradient-corrected (GGA) xc functional BP86 was used throughout.[25,26] For geometry optimization, the KS orbitals were represented with Gaussian-type basis sets used previously:[27] $(15s10p1d) \rightarrow [6s5p1d]$ for Mg cations and $(13s8p1d) \rightarrow [6s5p1d]$ for O anions. That oxygen basis set was also employed to describe electrons trapped by the oxygen vacancies. For the g-tensor calculations, the primitive orbital basis sets were extended and contracted in a special manner:[28] O $(13s8p7d) \rightarrow [8s7p3d]$, Mg $(15s10p9d) \rightarrow [8s9p3d]$. These basis sets were shown to be large enough to produce g values converged to better than 10^{-4}.[13] For the boundary Mg^{2+} cations (Mg^*), a very compact basis set was used in the spin-orbit calculations: $Mg^*(15s10p) \rightarrow [3s2p]$. During the geometry optimization, such Mg^* centers were described by pseudopotentials Mg^{ECP} without a basis set.[22] The auxiliary Gaussian-type basis set used to represent the electron charge density was constructed as described elsewhere[24] and augmented by standard sets of five p- and five d-type polarization functions on each atom.

In the calculations with the code GAUSSIAN03,[21] the Gaussian-type basis set 6-31G[29] on all Mg and O ions has been used to construct the KS orbitals; the more flexible 6-31G* basis set has been employed on the Mg atoms nearest to the vacancy to describe the electron localization in the cavity.[30] For the terrace (001) site, g tensors have been also computed for the optimized geometry using more flexible basis sets, 6-311+G* on Mg nearest to the vacancy (and 6-31G* on the other Mg)[29] and EPR-II on O.[31] To examine the effect of the xc functional on g values, we also applied the hybrid functional B3LYP.[32,33] With the GGA functional BP86, g tensors were computed in a single-point approach for the geometries optimized at the B3LYP level.

To construct the quantum-mechanical (QM) part of the cluster models of MgO, one takes a finite partition of the crystal lattice. This truncation is successful because of the highly ionic character of the material, but for an accurate

TABLE I. Sensitivity of the PARAGAUSS g and $\Delta g \equiv g - g_e (\times 10^5)$ values for F_s^+ centers on MgO(001) corner, edge, and terrace sites to positions of nearby Mg and O atoms.

Model	Geometry	g_{xx}	g_{yy}	g_{zz}	Δg_{xx}	Δg_{xx}	Δg_{zz}
Corner							
I	unrelaxed	2.017 40	2.017 40	2.002 35	1508	1508	3
II	equilibrium	2.000 22	2.000 22	2.001 18	−210	−210	−114
Edge							
III	unrelaxed	2.002 81	2.002 58	2.002 52	49	26	20
IV	equilibrium	2.000 66	2.000 99	2.001 36	−166	−133	−96
Terrace (001)							
V	unrelaxed[a]	2.003 48	2.003 48	2.004 70	116	116	238
VI	equilibrium[b]	2.001 01	2.001 01	2.001 76	−131	−131	−56
VII	**VI**, $r(Mg_4)$ of **V**	2.002 18	2.002 18	2.003 53	−14	−14	121
VIII	**VI**, $z(Mg_4)$ of **V**	2.002 16	2.002 16	2.003 51	−16	−16	119
IX	**VIII**, $z(Mg_1)$ of **V**	2.002 35	2.002 35	2.003 72	3	3	140
X	**IX**, $r+z(Mg_4$, second layer) of **V**	2.002 31	2.002 31	2.003 75	−1	−1	143
XI	**X**, $r+z(O_4)$ of **V**	2.003 01	2.003 01	2.004 40	69	69	208
XII	**XI**, $r+z(O_4$, second layer) of **V**	2.003 49	2.003 49	2.004 84	117	117	252

[a]Coordinates fixed as optimized for the regular MgO(001) surface in Ref. 22 (see Table II).
[b]Positions of all atoms of the F_s^+ center are optimized, Ref. 22 (see Table II).

model one has to include an external field that represents the long-range Coulomb potential. The close environment of the QM clusters was represented by its classical atomistic structure (of polarizable ions), optimized without constraints using a shell-model-type force field;[34] the shell-model region was surrounded by a large array of nonpolarizable ions (point charges). Mg ions at the interface between the QM cluster and the region of classical ions, Mg^{ECP}, were described by an effective core potential. All QM atoms and classical polarizable ions were allowed to relax during the geometry optimization. Details of the embedding procedures and the geometry optimization can be found elsewhere, for calculations with PARAGAUSS (Ref. 22) and GAUSSIAN03 interface with the GUESS code.[23] In spin-orbit PARAGAUSS calculations of g tensors the QM parts of the cluster models were $Mg_9O_8^+(Mg_{16}^*)$—(001) terrace, $Mg_6O_5^+(Mg_{10}^*)$—edge between (001) terraces, $Mg_4O_6^{5-}(Mg_9^*)$—corner; larger clusters were used during the corresponding geometry optimization: $Mg_9O_8^+(Mg_{16}^{ECP})$, $Mg_{16}O_{15}^+(Mg_{16}^{ECP})$, and $Mg_{10}O_9^+(Mg_{12}^{ECP})$, respectively. The QM parts of the cluster models of F_s^+ centers treated with GAUSSIAN03 were $Mg_{14}O_{13}^+(Mg_{16}^{ECP})$—(001) terrace, $Mg_{12}O_{11}^+(Mg_{14}^{ECP})$—edge between two terraces, $Mg_{10}O_9^+(Mg_9^{ECP})$—corner and $Mg_{11}O_{10}^+(Mg_{13}^{ECP})$—monatomic step on a (001) terrace.

The validity of the theoretical approach used has been checked by comparing the computed and measured g factor for a bulk F^+ center in MgO. This has been measured accurately, and coincides with the free electron value,[35] $g_e = 2.0023$. The calculations have been done with the GAUSSIAN03/GUESS codes, using a $Mg_{14}O_{18}^{9-}(Mg_{30}^{ECP})$ cluster, and the same basis set used for the surface F^+ centers 6-31G* on the Mg atoms nearest to the vacancy, 6-31G on the rest). The computed g factor, 2.002 53, differs by only $\approx$200 ppm from the experimental one, thus providing a solid validation of the computational approach.

III. RESULTS AND DISCUSSION

The structure of charged surface color centers on MgO, F_s^+, even on the (001) terraces,[22] undergoes a rather significant relaxation compared to the geometry preceding the formation of the vacancy. Thus, in a first step, we will address how sensitive g tensors of F_s^+ centers are with respect to structure parameters.

In Table I, we compare g values calculated with PARAGAUSS for unrelaxed F_s^+ centers (i.e., held at the geometry optimized without a vacancy) at corner, edge, and (001) terrace sites of MgO with the values of the corresponding relaxed centers, i.e., with atoms at equilibrium (optimized) positions. One immediately notices that for all considered unrelaxed geometries of corner (I), edge (III), and terrace (V) sites all shifts Δg with respect to the free-electron value g_e are *positive*, i.e., $g > g_e$. Also, model I exhibits quite a significant g-tensor anisotropy, $\sim$0.015, whereas almost isotropic g tensors are calculated for the models III and V. When relaxation to the corresponding equilibrium geometries II, IV, and VI is allowed, g-tensor signatures of all the centers under scrutiny are changed dramatically: all g components become smaller than g_e and the anisotropy reduces to <0.001.

To better understand this strong structural dependence, we examined more closely models V and VI of F_s^+ center on a (001) terrace. As follows from Table II, the most prominent relaxation effect of VI with respect to V is an outward [almost parallel to the (001) plane] displacement of the four Mg^{2+} nearest neighbors of the vacancy, by 15 pm. This structural change is mainly driven by a (relative) destabilization as the repulsive Mg^{2+}–Mg^{2+} interactions within the upper Mg_4 moiety of the QM cluster $Mg_9O_8^+(Mg_{16}^{ECP})$ are stronger than those in the presence of the central O anion; concomitantly, the Mg_1 cation on the C_4 symmetry axis in the sub-

TABLE II. Axial (r) and vertical (z) positions (all distances in picometer, z "upward" displacement of upper-layer Mg_4 and O_4 ions relative to the structure of bulk terminated MgO) of Mg and O atoms closest to F_s^+ centers on MgO(001) terraces for structures calculated with PARAGAUSS unrelaxed geometry [taken as on the defect-free (001) surface, model **V**] and in the optimized equilibrium geometry, model **VI** (see Table I).

Distance	Geometry		
	Unrelaxed	Equilibrium[a]	
$r(Mg_4)$	211	226	(232)
$z(Mg_4)$	3	7	(5)
$r(O_4)$	299	291	(295)
$z(O_4)$	11	16	(5)
$z(Mg_1)$	−206	−212	(−219)
$r(O_4$, second layer)	212	209	(210)
$z(O_4$, second layer)	−208	−201	(−210)

[a]Structure data as obtained with GUESS code are given in parentheses.

surface layer moves "down" to elongate the distances to the cations of the "upper" Mg_4 unit. The O_4 shell of anions in the surface layer experiences the next largest displacement; these centers move inward by 8 pm. All these displacements contribute to make the cavity of the F_s^+ center on the (001) terrace more "round" in the equilibrium structure VI than in the unrelaxed model V. Overall, going from V to VI, we calculated a notable decrease of g values, by -247×10^{-5} for $g_\perp \equiv g_{xx}=g_{yy}$ and -294×10^{-5} for $g_\parallel \equiv g_{zz}$ (Table I); as a result, both components of the axial tensor, $g_\perp$ and $g_\parallel$ become smaller than the free-electron value g_e.

Using a linear extrapolation of the slope $\partial g/\partial\Delta r(Mg_4)$ obtained for structure VI, we estimate that the relocation of the Mg_4 ions of structure VI to their axial positions in the structure V by $\Delta r(Mg_4)=-15$ pm (Table II) is accompanied by an increase of $g_\perp$ by 83×10^{-5} and of $g_\parallel$ by 143×10^{-5}; the corresponding changes, calculated explicitly when going from the structure VI to VII (Table I), are 117×10^{-5} and 177×10^{-5}, respectively. Note that the latter alteration due to $r(Mg_4)$ alone is, in fact, responsible for half of the calculated overall g-tensor change between the relaxed (VI) and unrelaxed (V) models of terrace F_s^+ centers. Further partial displacements of Mg_4 (VIII), Mg_1 (IX), (Mg_4, second layer) (X), O_4 (XI), and (O_4, second layer) (XII) finally result in $\Delta g_\perp=117\times10^{-5}$ and $\Delta g_\parallel=252\times10^{-5}$ (Table I), which are very close to $\Delta g_\perp=116\times10^{-5}$ and $\Delta g_\parallel=238\times10^{-5}$, computed for the completely unrelaxed model V. This agreement holds despite that in the latter model all Mg^* cations of the QM region as well as the whole set of the surrounding classical ions remained at their positions of the relaxed structure VI.

This analysis shows that the g tensor of F_s^+ centers (and thus the behavior of the unpaired electron in the vacancy) is basically determined by the positions of the Mg and O ions closest to the vacancy. Positions of more distant ions and details of the Madelung field are of only minor importance. Therefore, it seems that the g tensor provides a rather local probe of F_s^+ centers on the (001) terrace of MgO. The equilibrium structures of this center computed with PARAGAUSS and GAUSSIAN03/GUESS (Table II) differ at most by 10 pm in various individual coordinates. From test calculations with PARAGAUSS of the above two equilibrium geometries, we estimate the uncertainty of g tensors caused by structure differences as a consequence of the two computational schemes (embedding, cluster size, basis set, xc, etc.) at 5×10^{-5} only (Table III). To conclude the discussion of relaxation effects on g tensors of the three different F_s^+ centers listed in Table I, we would like to reiterate that, for an adequate representation of g values, it is crucial to take structure relaxation into ac-

TABLE III. g and $\Delta g \equiv g-g_e(\times10^5)$ values for various F_s^+ centers on MgO (see Fig. 1) as calculated with PARAGAUSS and GAUSSIAN03 using the xc functionals BP86 and B3LYP. Also shown are experimental values for ordered MgO(001) films.

Site	Method	g_{xx}	g_{yy}	g_{zz}	Δg_{xx}	Δg_{yy}	Δg_{zz}
Corner	PARAGAUSS, BP86	2.000 22	2.000 22	2.001 18	−210	−210	−114
	GAUSSIAN, BP86[a]	1.999 86	1.999 85	2.001 76	−246	−247	−56
	GAUSSIAN, B3LYP	2.000 15	2.000 15	2.001 85	−217	−217	−47
	Expt.[b]	1.999 97	1.999 97	2.000 37	−236	−236	−195
Edge[c]	PARAGAUSS, BP86	2.000 66	2.000 99	2.001 36	−166	−133	−96
	GAUSSIAN, BP86[a]	2.000 29	2.000 77	2.001 37	−203	−155	−95
	GAUSSIAN, B3LYP	2.000 53	2.000 99	2.001 47	−179	−133	−85
	Expt.[b]	1.999 85	1.999 95	2.000 50	−247	−237	−182
Step[c]	GAUSSIAN, BP86[a]	2.000 49	2.000 87	2.001 18	−183	−145	−114
	GAUSSIAN, B3LYP	2.000 76	2.001 07	2.001 31	−156	−125	−101
	Expt.[b]	1.999 95	2.000 09	2.000 24	−237	−223	−208
Terrace(001)	PARAGAUSS, BP86	2.001 01	2.001 01	2.001 76	−131	−131	−56
	PARAGAUSS, BP86[a]	2.001 04	2.001 04	2.001 70	−128	−128	−62
	GAUSSIAN, BP86[a]	2.000 76	2.000 76	2.002 02	−156	−156	−30
	GAUSSIAN, B3LYP	2.000 95	2.000 95	2.002 07	−137	−137	−25
	GAUSSIAN, B3LYP[d]	2.000 91	2.000 91	2.002 11	−141	−141	−21

[a]Geometry optimized with B3LYP xc functional (see Table II).
[b]Experimental values (error bar ±0.000 05) from Ref. 9. For step site, reevaluated (see text).
[c]The y axis is oriented along the edge.
[d]Basis set for Mg atoms surrounding the O vacancy extended from the standard 6-31G* to 6-311+G*; for the other Mg atoms from 6-31G to 6-31G*; for O atoms from the standard 6-31G to EPR-II.

count in a sufficiently accurate fashion. As will be shown below, only with such sophisticated models it is possible to reach agreement with experimental results.[9] Before dealing with experimental data, let us briefly examine the g values, calculated using different tools and approximations.

In Table III we display g values (and the corresponding shifts $\Delta g \times 10^5$) for F_s^+ centers on MgO corners, edges, steps as well as (001) terraces as calculated with PARAGAUSS and GAUSSIAN03. For example, g values at the BP86 level calculated for the corner site with the two codes vary at most by 0.0006 for the parallel component; for the perpendicular g components the difference is even smaller—despite notable methodological differences between these computational approaches: different cluster models and embedding, relativistic versus nonrelativistic treatment of KS eigenfunctions, spin-orbit effect included self-consistently, or perturbatively, different basis sets. Switching from a BP86-GGA xc functional to the hybrid B3LYP approach results in a change in g values of at most 0.0003. Similar uncertainties also hold for F_s^+ centers at other positions under scrutiny. Table III also documents that the GAUSSIAN03 g values are stable to 0.000 04 or better with respect to an extension of the basis set. In summary, the g values calculated with the present two different computational schemes are consistent at least to three digits. The accuracy is higher, when one discusses relative g values in a series of similar systems, calculated with the same approach.

Of special importance is the result that the same g factors are obtained with different xc functionals, in particular, when comparing BP86 results with the hybrid B3LYP approach. The extent of electrons and holes localization in insulators depends significantly on the level of treatment, giving more delocalized descriptions with pure DFT functionals.[36] This is the consequence of the self-interaction problem, which is reduced by mixing single-determinant exact exchange and a (semi) local exchange functional, as done in hybrid functionals. The fact that BP86 and B3LYP give similar results suggests that the g factor is much less sensitive to the form of the functional compared, for instance, to hyperfine coupling constants.[36]

Next, we address the question how accurately the calculated g values represent experimental EPR data for F_s^+ centers on MgO. To this end, we compare the former with recently determined experimental results for corner and edge (step) paramagnetic color centers generated by electron bombardment on well-ordered crystalline MgO thin films grown on Mo(100) (Ref. 9) (Table III). The measured g shifts are small, *negative* (see the discussion of the cluster relaxation effect above in this section), and they exhibit a small anisotropy. For the corner site, our model with C_{3v} symmetry implies an axial g tensor; the calculated and detected $g_\perp$ values agree essentially quantitatively, whereas the calculated shifts $\Delta g_\parallel$ somewhat underestimate the experimental value, with the direction of the $g_\parallel$ component coinciding with the C_3 symmetry axis. Thus, the calculated anisotropy of the g tensor is slightly larger than in experiment. For the edge center the general picture is rather similar; the calculated shifts $\Delta g_\perp$ and $\Delta g_\parallel$ underestimate (in absolute terms) the experimental values very slightly and nearly by the same amount. As a consequence, the calculated g-tensor anisotropy fits closely the measured one. The calculated negative shift of g_{xx} is slightly larger, by 0.0003–0.0006, than the shift of g_{yy}. The resulting y and x directions point along the edge and normal to the plane spanned by the C_{2v} axis and the edge, respectively. F_s^+ centers at edge sites and at monoatomic steps show similar g_{xx} and g_{yy} values, differing at most by 0.0002 (for the same xc potential), with edge sites presenting smaller values. The opposite trend is found for the g_{zz} values which are larger for the edge sites by at most 0.0002. These small changes in the g-tensor components may be expected on the basis of the structural similarity of the types of vacancies at edges and steps; still the differences between F_s^+ centers formed at these sites are significant since they represent about 50% of the experimentally observed effect. However, there is an additional important difference between the two sites. In the case of a F_s^+ center on the ideal edge the direction of the g_{zz} component coincides with the C_{2v} symmetry axis of the edge (g_{yy} is oriented along the edge). For the step edge the g_{yy} direction remains collinear with the direction of the edge due to symmetry reasons, but the angle between the direction of g_{zz} and the surface normal is now 28° corresponding to a rotation of 17° form the "virtual" C_{2v} axis towards the surface normal, Fig. 2. Notice that the angle of 17° is deduced assuming that the direction of g_{zz} component goes exactly through the edge; in fact, there is a very small displacement and the actual angle is 22°, see Fig. 2.

This has also consequences for the analysis of the experimental data where it was originally assumed that the

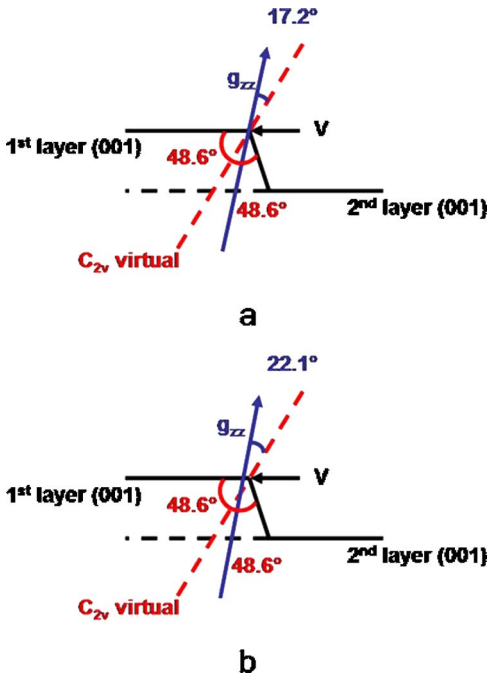

FIG. 2. (Color online) Direction of the g_{zz} component for a step site as obtained from DF calculations (side view): (a) assuming that g_{zz} goes exactly through the step edge (point V) the angle formed between g_{zz} and the "virtual" C_{2v} axis is 17.2°; (b) taking the exact direction, where g_{zz} is slightly displaced from the step edge, the angle is 22.1°. Notice that the geometrical relaxation changes the angle at the step edge from 90° (truncated bulk) to $48.6° \times 2 = 97.2°$.

color center is located at an ideal edge.[9] The information on the directions of the *g*-tensor components for the more realistic monoatomic step permits a reevaluation of the experimental data. The result of this analysis using the experimental data presented in Ref. 9 is given in Table III. It is interesting to note that the new fit, obtained using the 22° angle of g_{zz}, is slightly better than the one to the ideal edge, even though it would not be possible to justify the lift of the C_{2v} symmetry on the basis of the experimental data. In addition, the values extracted from the experiment show the same behavior as the theoretical data when going from ideal edges to step edges. The values of g_{xx} and g_{yy} increase, while g_{zz} decreases for the step edge. However, the deviation between theoretical and experimental values remains almost unchanged indicating that some systematic deviation may still exist.

To this end it is interesting to note that all calculated *g* shifts *underestimate* (in absolute terms) the corresponding experimental data. This is at variance with earlier PARAGAUSS results for radicals formed by atoms of *sp* elements;[13] those calculated *g* shifts were systematically moderately larger (in absolute value) than the measured results. This latter deficiency has been assigned to the overestimation of spin-orbit interaction at the DKH level in those paramagnetic molecules, even when one accounts for the electron-electron screening of spin-orbit interaction.[13,37] Therefore, *g* tensors of vacancies made up by ions of *sp* type with one trapped electron differ from those of molecular *sp* radicals; indeed, instead of a nucleus at the F center, one has only overlapping tails of nearby nuclear potentials.

Thus far it has not been possible to record *g* shifts in EPR signals of F_s^+ centers on terrace sites of ordered MgO samples. Therefore, the calculated results listed in Table III for color centers on the (001) terraces are predictions. Accordingly, this defect should be characterized by an axial *g* tensor that is sufficiently different from the orthorhombic *g* tensors of defects at edge (step) sites, discussed above irrespective of the model studied (Table III). F_s^+ centers on extended (001) terraces are predicted to feature g_{iso} values $\sim$0.0003 larger than those at edges (steps). Thus, it should be possible to differentiate these species experimentally provided they can be prepared at sufficiently high concentration.

IV. CONCLUSIONS

We reported a high-level theoretical description of EPR *g* tensors of surface color centers F_s^+ located at various positions of MgO: on (001) terraces as well as at steps, edges, and corners. To this end, we studied a series of cluster models optimized when consistently embedded in a polarizable environment by means of two independently developed advanced embedding schemes. To compute *g* tensors, we also employed two different DF approaches: one taking spin-orbit interaction self-consistently into account and another one relying on a perturbation treatment of spin-orbit interaction. Despite of these notable methodological differences, *g* tensors of the same type of F_s^+ centers, obtained with the alternative computational approaches, turned out to be very similar, showing only a weak dependence on the exchange-correlation functional. However, we encountered a dramatic sensitivity of calculated *g* values on the structure of F_s^+ centers; relaxation even reversed the sign of $\Delta g \equiv g - g_e$. We analyzed this effect in terms of individual displacements of the atoms constituting the color center. This strong structural sensitivity appears to limit the accuracy of calculated *g* values of F_s^+ centers on MgO.

Calculated *g* tensors of all F_s^+ sites studied exhibit rather small anisotropies and very small *negative* shifts Δg, in line with experimental *g*-tensor patterns of edge (step) and corner F_s^+ centers, recently measured under UHV conditions on single-crystalline MgO film.[9] Our calculations provided information on the direction of the main axes of *g* tensors on edge and step sites, and permitted a reevaluation of the original experimental data with a more realistic structural model, namely, a monoatomic step edge. The extracted *g*-tensor components show the same qualitative behavior when going from ideal edges to a step edge as predicted by theory. We also predicted *g*-tensor patterns for F_s^+ centers on the MgO (001) terrace sites, not yet detected experimentally. In general, the present study demonstrates that calculated *g* tensors are sufficiently accurate to assist in the precise EPR characterization of paramagnetic color centers on oxide surfaces. This provides additional evidence about the nature and the structure of the color centers formed by electron bombardment at the surface of MgO thin films.

ACKNOWLEDGMENTS

This work was supported by the Spanish Ministry of Education and Science (CTQ2005-08459-C02-01), Generalitat de Catalunya (2005SGR00697), Italian Ministry of Research through a Cofin 2003 project, EU through the STREP program GSOMEN, Deutsche Forschungsgemeinschaft, Fonds der Chemischen Industrie, Volkswagen Foundation, and by the Alexander von Humboldt Foundation through the institute partnership program. M.S. is grateful to the Austrian Science Fund (FWF) for financial support. This work is dedicated to Professor Volker Staemmler on the occasion of his 65th birthday.

[1] G. Pacchioni, ChemPhysChem **4**, 1041 (2003).
[2] R. Schaub, E. Wahlström, A. Rønnau, E. Laesgaard, I. Stensgaard, and F. Besenbacher, Science **299**, 377 (2003).
[3] A. Abragam and B. Bleaney, *Electron Paramagnetic Resonance of Transition Ions* (Clarendon, Oxford, 1970).
[4] E. Giamello, M. C. Paganini, D. M. Murphy, A. M. Ferrari, and G. Pacchioni, J. Phys. Chem. B **101**, 971 (1997).
[5] M. Chiesa, M. C. Paganini, G. Spoto, E. Giamello, C. Di Valentin, A. Del Vitto, and G. Pacchioni, J. Phys. Chem. B **109**, 7314 (2005).
[6] T. Berger, M. Sterrer, O. Diwald, and E. Knözinger, J. Phys. Chem. B **108**, 7280 (2004).
[7] A. Kolmakov, J. Stultz, and D. W. Goodman, J. Chem. Phys. **113**, 7564 (2000).
[8] J. Kramer, C. Tegenkamp, and H. Pfnür, Phys. Rev. B **67**, 235401 (2003).
[9] M. Sterrer, E. Fischbach, T. Risse, and H.-J. Freund, Phys. Rev. Lett. **94**, 186101 (2005).
[10] D. Stehlik and K. Möbius, Annu. Rev. Phys. Chem. **48**, 745 (1997).
[11] K. Möbius, A. Savitsky, A. Schnegg, M. Plato, and M. Fuchs, Phys. Chem. Chem. Phys. **7**, 19 (2005).
[12] J. E. Harriman, *Theoretical Foundations of Electron Spin Resonance* (Academic, New York, 1978).
[13] K. M. Neyman, D. I. Ganyushin, A. V. Matveev, and V. A. Nasluzov, J.

Phys. Chem. A **106**, 5022 (2002).
[14] T. Belling, T. Grauschopf, S. Krüger, M. Mayer, F. Nörtemann, M. Staufer, C. Zenger, and N. Rösch, in *High Performance Scientific and Engineering Computing*, Lecture Notes in Computational Science and Engineering Vol. 8, edited by H.-J. Bungartz, F. Durst, and C. Zenger (Springer, Heidelberg, 1999), p. 439.
[15] T. Rösch *et al.*, PARAGAUSS, Version 3.0, Technische Universität München, Munich, 2004.
[16] M. Mayer, S. Krüger, and N. Rösch, J. Chem. Phys. **115**, 4411 (2001).
[17] M. Douglas and N. M. Kroll, Ann. Phys. **82**, 89 (1974).
[18] B. A. Hess, R. J. Buenker, and P. Chandra, Int. J. Quantum Chem. **29**, 737 (1986).
[19] N. Rösch, S. Krüger, M. Mayer, and V. A. Nasluzov, in *Recent Developments and Applications of Modern Density Functional Theory*, Theoretical and Computational Chemistry Series Vol. 4, edited by J. M. Seminario (Elsevier, Amsterdam, 1996), p. 497.
[20] F. Neese, J. Chem. Phys. **115**, 11080 (2001).
[21] M. J. Frisch *et al.*, GAUSSIAN03, Revision A.7, Gaussian Inc., Pittsburgh, PA, 2003.
[22] V. A. Nasluzov, V. V. Rivanenkov, A. B. Gordienko, K. M. Neyman, U. Birkenheuer, and N. Rösch, J. Chem. Phys. **115**, 8157 (2001).
[23] P. V. Sushko, A. L. Shluger, and C. R. A. Catlow, Surf. Sci. **450**, 153 (2000).
[24] B. Dunlap and N. Rösch, Adv. Quantum Chem. **21**, 317 (1990).
[25] A. D. Becke, Phys. Rev. A **38**, 3098 (1988).
[26] J. P. Perdew, Phys. Rev. B **33**, 8822 (1986); **34**, 7406 (1986).
[27] K. M. Neyman, C. Inntam, A. V. Matveev, V. A. Nasluzov, and N. Rösch, J. Am. Chem. Soc. **127**, 11652 (2005).
[28] K. M. Neyman, D. I. Ganyushin, V. A. Nasluzov, N. Rösch, A. Pöppl, and M. Hartmann, Phys. Chem. Chem. Phys. **5**, 2429 (2003).
[29] R. Ditchfeld, W. Hehre, and J. A. Pople, J. Chem. Phys. **54**, 724 (1971).
[30] R. Soave, A. M. Ferrari, and G. Pacchioni, J. Phys. Chem. B **105**, 9798 (2001).
[31] V. Barone, in *Recent Advances in Density Functional Methods*, edited by D. P. Chong (World Scientific, Singapore, 1996), p I.
[32] A. D. Becke, J. Chem. Phys. **98**, 5648 (1993).
[33] C. Lee, W. Yang, and R. G. Parr, Phys. Rev. B **37**, 785 (1988).
[34] G. V. Lewis and C. R. A. Catlow, J. Phys. C **18**, 1149 (1985).
[35] J. E. Wertz, P. Auzins, R. A. Weeks, and R. H. Silsbee, Phys. Rev. **107**, 1535 (1957).
[36] G. Pacchioni, F. Frigoli, D. Ricci, and J. A. Weil, Phys. Rev. B **63**, 054102 (2001).
[37] K. M. Neyman, D. I. Ganyushin, Ž. Rinkevičius, and N. Rösch, Int. J. Quantum Chem. **90**, 1404 (2002).